Desalination and Water Treatment

ISSN: 1944-3994 (Print) 1944-3986 (Online) Journal homepage: http://www.tandfonline.com/loi/tdwt20

Adsorption behavior of chromium(VI) on activated carbon from eucalyptus sawdust prepared by microwave-assisted activation with $ZnCl_2$

Congjin Chen, Pengcheng Zhao, Zhixia Li & Zhangfa Tong

To cite this article: Congjin Chen, Pengcheng Zhao, Zhixia Li & Zhangfa Tong (2016) Adsorption behavior of chromium(VI) on activated carbon from eucalyptus sawdust prepared by microwave-assisted activation with $ZnCl_2$, Desalination and Water Treatment, 57:27, 12572-12584, DOI: 10.1080/19443994.2015.1049960

To link to this article: http://dx.doi.org/10.1080/19443994.2015.1049960

Published online: 28 May 2015.

Desalination and Water Treatment
www.deswater.com
doi: 10.1080/19443994.2015.1049960

57 (2016) 12572–12584
June

Taylor & Francis
Taylor & Francis Group

Adsorption behavior of chromium(VI) on activated carbon from eucalyptus sawdust prepared by microwave-assisted activation with $ZnCl_2$

Congjin Chen[a,b,*], Pengcheng Zhao[a], Zhixia Li[a], Zhangfa Tong[a,b,*]

[a]*School of Chemistry and Chemical Engineering, Guangxi University, Nanning 530004, China, Tel./Fax: +86 7713233718; emails: gxdxccj@163.com, chencongjin@gxu.edu.cn (C. Chen), Tel./Fax: +86 7713239697; emails: zhftong@sina.com, dean@gxu.edu.cn (Z. Tong)*
[b]*Guangxi Key Laboratory of Petrochemical Resource Processing and Process Intensification Technology, Guangxi University, Nanning 530004, China*

Received 15 October 2014; Accepted 5 May 2015

ABSTRACT

Activated carbon (AC) was prepared from eucalyptus sawdust by microwave-assisted activation with $ZnCl_2$ and utilized for removing chromium(VI) from an aqueous solution with a concentration of 10–80 mg L^{-1} and a temperature of 30–60°C. The effects of pH, contact time, initial concentration of Cr(VI) and temperature on adsorption, as well as the thermodynamics and kinetics were investigated. The results were as follows: (1) The adsorption capacity of Cr(VI) was dependent on pH and initial concentration as the equilibrium time increased, but the Cr(VI) removal percentage decreased with an increase in the initial Cr(VI) concentration; (2) The adsorption process was in good agreement with the Langmuir adsorption isotherm model at 30°C and the Freundlich adsorption isotherm model at 45 and 60°C; (3) Adsorption thermodynamic parameters ΔH°, ΔS°, and ΔG° indicated that Cr(VI) adsorption on AC was a spontaneous and endothermic process with increased randomness at the solid–solution interface; (4) Cr(VI) adsorption on AC followed a pseudo-second-order equation at 30, 45, and 60°C fitted into an intraparticle diffusion model at 30 and 45°C, and it followed a pseudo-first-order equation only at 60°C and at Cr(VI) concentrations of 10 and 20 mg L^{-1}.

Keywords: Activated carbon; Cr(VI) adsorption; Isotherms model; Adsorption thermodynamics parameters; Adsorption kinetics model

1. Introduction

Heavy metal contamination is one of the world's most noteworthy environmental problems. The increasing use of chromium chemicals in many industrial processes, such as leather tanning, mining of chrome ore, production of steel and alloys, dyes and pigment manufacturing, the glass industry, wood preservation, the textile industry, film and photography, metal cleaning, plating and electroplating, has led to large amounts of polluted aqueous effluents that contain high levels of chromium [1,2]. In natural waters, the range of chromium concentrations is quite large, from 5.2 to 208,000 mg L^{-1} [1,3]. Nevertheless, for most natural waters, the Cr concentration is below the 50 μg L^{-1} value recommended for drinking water

*Corresponding authors.

by the World Health Organization or the US Environmental Protection Agency [1,4,5].

Chromium can exist at six different oxidation states, as with most transition metals, but in the Eh–pH range of natural water, the only important ones are trivalent Cr(III) and hexavalent Cr(VI) [1,3,6]. Of these two, Cr(VI) is highly toxic to humans, plants, and animals. Cr(VI) is the most toxic form, being carcinogenic and mutagenic to living organisms [1,7]. In addition, it leads to liver damage, pulmonary congestion and causes skin irritation resulting in ulcer formation [1,8]. Trivalent Cr(III) is approximately 300 times less toxic than Cr(VI), and because it has limited hydroxide solubility, it is less mobile and less bioavailable [1,9]. Cr(III) is essential to animals and plants and plays an important role in sugar and fat metabolism, although in excess, it can cause allergic skin reactions and cancer [1,10]. Therefore, high concentration of Cr(VI) ions should be reduced to acceptable levels before discharging into the environment. Various technologies, such as precipitation [11], membrane filtration [12], solvent extraction with amines [13], ion exchange [14], electro deposition [15,16] and biological processes [17], activated carbon (AC), and low-cost adsorbents adsorption [6,18], have been developed to remove Cr(VI) ions from aqueous solution. Among them, the adsorption process may be an effective and promising technique to achieve the targeted degree of removal, recovery, and recycling of Cr(VI) ions in aqueous solution [19].

AC is a reproducible and multi-porous adsorbent. It is a carbon-containing substance with a developed pore structure, high specific surface area, good adsorption capacity, thermo-stability, and low acid/base reactivity characteristics [20,21]. Based on these unique properties, AC is applied in almost all fields and is particularly useful in dealing with pollutants [21–23]. AC adsorption has been widely used for the treatment of chromium-containing wastewaters [24–29]. However, commercially available AC may be expensive, and for this reason, any cheap material, with a high carbon content and low inorganic content, can be used as a raw material for the production of AC. Wood production has significantly increased in China over the last decade, and eucalyptus is widely planted in south China. Wood processing and appropriate maintenance of forests generate a considerable volume of eucalyptus woody residues. One potential application of wood waste is as raw material for charcoal and AC production.

In this study, AC from eucalyptus sawdust (ES) was produced by microwave-assisted chemical activation with $ZnCl_2$ and characterized, and the adsorption isotherms, thermodynamics and kinetics process and relative parameters of Cr(VI) adsorption on ESAC were investigated.

2. Materials and methods

2.1. Reagents

Zinc chloride ($ZnCl_2$), methylene blue ($C_{16}H_{18}N_3SCl$), phenol (C_6H_5OH), hydrochloric acid (37% HCl), iodine (I_2), potassium iodide (KI), sodium thiosulfate ($Na_2S_2O_3$), sodium carbonate (Na_2CO_3), potassium dichromate ($K_2Cr_2O_7$), copper sulfate ($CuSO_4{\cdot}5H_2O$), sodium phosphate dibasic (NaH_2PO_4), potassium dihydrogen phosphate (KH_2PO_4), diphenylcarbazide ($C_{13}H_{14}N_4O$), and acetone (C_3H_6O) were purchased from the Shanghai Sinopharm Chemical Reagent Company Ltd (Shanghai, China). All chemicals were of analytical grade and produced in the Spark Chemical Plant, Pudong New Area, Shanghai.

2.2. AC preparation and characterization

The raw material, *Eucalyptus grandis* sawdust, was provided by the Guangxi Gaofeng Farm, China, selected with particles of 0.25–0.42 mm by sieving. The standard methods for the proximate analysis of solid biofuels GB/T 28731-2012 (China) was used to characterize the ES. The material contained 83.25% volatile matter, 9.2% fixed carbon, 0.67% ash, and 6.88% moisture [30].

ES (30.00 g) with a particle size between 0.25 and 0.42 mm was mixed with a $ZnCl_2$ aqueous solution (50% mass concentration, pH 3) at a mass ratio ($ZnCl_2$: ES) of 2:1. After being impregnated for 24 h in a quartz reactor, the sample was subjected to microwave-assisted carbonization and activation for 28 min with power of 800 W using a modified WD800 (MG-5334MV) LG microwave oven (800 W, 2,450 MHz, Life's Good Co. Ltd, China). The prepared materials were cooled to room temperature and washed with hot hydrochloric acid (1.0 mol L^{-1}) and deionized water until the pH was approximately 6–7. The AC was filtered, dried at 110°C for 24 h, and stored in tightly closed bottles until further analysis. The yield (Y) of the prepared AC was estimated from Eq. (1):

$$Y(\%) = \frac{M_{AC}}{M_0} \times 100 \quad (1)$$

where M_{AC} is the weight of the obtained AC, and M_0 is the weight of the dried EC.

The iodine number, methylene blue, and phenol adsorption capacity were determined according to the

national standard of the people's Republic of China GB/T 12496.8-1999, GB/T 12496.10-1999, and GB/T 12496.12-1999 (standard test methods of wooden AC in China). The Cr(VI) adsorption capacity of AC was based on the change in Cr(VI) concentration after contact with 0.1 g AC with a Cr(VI) aqueous solution (V = 20 mL, C_0 = 100 mg L^{-1}, natural solution pH, and room temperature) at 120 rpm for 60 min. The Cr(VI) concentration was determined with the 1,5-diphenyl carbazide method followed by spectrophotometric determination at 540 nm [31,32] using a UV/VIS2802PCS spectrophotometer (Unico Instrument Co., Ltd, Shanghai, China). The amount q_t (mg g^{-1}) of adsorbed Cr(VI) on AC was calculated by Eq. (2)

$$q_{t(e)} = \frac{(C_0 - C_{t(e)})V}{1,000 \times M_{AC}} \quad (2)$$

where C_0, C_t, and C_e are the initial, remaining, and equilibrium concentrations (mg L^{-1}) of Cr(VI) solution, respectively, V is the volume of the Cr(VI) aqueous solutions (mL), and M_{AC} is the weight of added AC (g).

The pore properties of AC were characterized by N_2 adsorption–desorption isotherms and the Brunauer–Emmett–Teller (BET) equation. The organic functional groups on the surface of the ACs were identified by a Nicolet 6700 Fourier transform infrared spectrometer (FT-IR) (American Nicolet Corp.) and analyzed with OMNIC software.

2.3. Batch adsorption studies

Industrial wastewater containing chromium ions was simulated with a $K_2Cr_2O_7$ aqueous solution in this study. A stock solution (1,000 mg L^{-1}) of Cr(VI) was prepared by dissolving a precise quantity of $K_2Cr_2O_7$ (0.2829 g) in 1,000 mL of deionized water. The stock solution was diluted with deionized water to obtain the working solutions, and the concentration ranged from 10 to 100 mg L^{-1}.

The adsorption experiments were conducted using the batch technique. Batch adsorption experiments were performed by oscillating at 120 rpm in contact with 0.1 g AC with 20 mL of the aqueous solution of different initial Cr(VI) concentrations (10, 20, 40, and 80 mg L^{-1}). The pH adjustments of the Cr(VI) solutions were made using 0.1 mol L^{-1} HCl or 0.1 mol L^{-1} NaOH solutions. The pH was measured using a PHS-3C pH meter. Experiments were performed in a thermal shaker at different controlled temperatures (30, 45, and 60 ± 2°C) for desired times (60 or 120 min) using 50-mL tapered bottles with ground glass stoppers. The remaining concentration of Cr(VI) after adsorption at different time intervals was determined after filtering the AC with neutral filter paper. A batch process was used so that there was no need for volume correction. The adsorption capacity (mg g^{-1}) and the percentage removal (%) of Cr(VI) in the solution were calculated by Eqs. (2) and (3).

$$p_t\ (\%) = \frac{(C_0 - C_e)}{C_0} \times 100 \quad (3)$$

3. Results and discussion

3.1. Characterization of the prepared AC

The prepared AC yield was 32.0%. The methylene blue adsorption capacity, iodine number, phenol adsorption capacity, Cr(VI) adsorption capacity, and BET surface area of the prepared AC were 277.5, 1,041.5, 104.3, 6.29, and 1,429.4 m g^{-1}, respectively. The total pore volume, micropore volume, and average pore diameter of AC were 1.105, 0.008403 cm^3 g^{-1} and 3.09 nm, respectively. The prepared AC was of mesoporous structure which contained plenty of mesopores, macropores, and few micropores. Carbonyl and hydroxyl groups were found on the AC surface.

3.2. The thermodynamics study results of chromium(VI) adsorption on the prepared AC

3.2.1. Effect of pH

AC showed amphoteric character depending on the pH of the solution, i.e., the surface might be positively or negatively charged. The pore wall of the AC contained a large number of surface functional groups. The pH dependence of Cr(VI) adsorption was mainly related to the type and ionic state of these functional groups and adsorbate chemistry in the solution. Solution pH is an important parameter for the removal of heavy metals because it affects the solubility of adsorbates, concentration of the counter ions on the functional groups of the adsorbent and the degree of ionization of the adsorbate during reaction [33]. Chromium(VI) adsorption was studied as a function of pH over a range of 2.0–8.0 (Fig. 1). It was clear that the prepared AC was more active in the acidic range and that the maximum adsorption occurred at a pH 2.0. There was a sharp decrease in the sorption capacity when the pH was raised from 2.0 to 6.0; the effect then became negligible with a further increase. Chromium(VI) may exist in three different ionic forms ($HCrO^{4-}$, $Cr_2O_7^{2-}$ and CrO_4^{2-}) in aqueous solutions, and the stability of these ions in

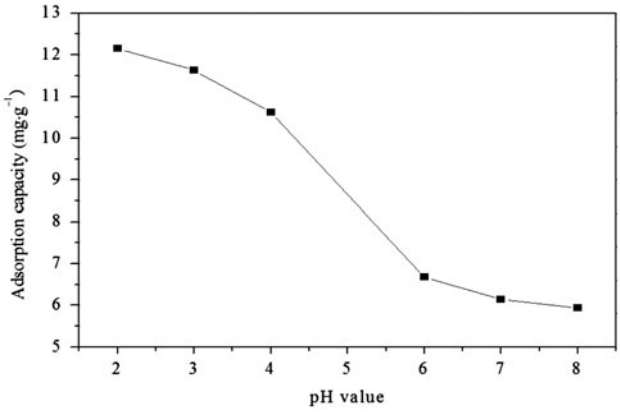

Fig. 1. The chromium(VI) adsorption capacity of AC under different pH values.

aqueous systems was mainly pH dependent [34]. The sorption capacity of Cr(VI) was higher in the lower pH range due to a high electrostatic force of attraction. As the number of H^+ ions increased with decreasing pH, the negative charge on the adsorbent surface was neutralized, and as a result, diffusion of chromate ions into the bulk of the adsorbent was increased [35]. As reported by other studies, Cr(VI) was adsorbed on the surface of AC mostly in the form of $HCrO^{4-}$ [36]. The decrease in the adsorption with increasing pH may be attributed to the increased number of OH^- ions in the bulk, which retarded the diffusion of chromate ions, such as $HCrO^{4-}$, $Cr_2O_7^{2-}$, and CrO_4^{2-}, and the competitiveness sorption of these oxyanions of Cr. However, Cr ions in a natural aquatic environment, such as drinking water sources, mostly exist at natural pH levels, and further studies of Cr(VI) adsorption on the prepared AC under natural pH conditions will be conducted.

3.2.2. Effect of contact time and initial concentration

The amount of Cr(VI) adsorbed on the AC was studied as a function of shaking time at four different initial concentrations (10, 20, 40, and 80 mg L^{-1}) of Cr (VI) and different temperatures (30 ± 2, 45 ± 2, and 60 ± 2°C). The results are given in Fig. 2 (a for 30°C, b for 45°C, and c for 60°C), respectively. These adsorption curves showed the relationship between the amounts of Cr(VI) adsorbed (q_t) and its contact time (t). It is evident from these figures that the adsorptivity of Cr(VI) increased with increase in contact time from 0 to 30 min and was almost saturated after 50 min. The initial concentrations of Cr(VI) and the absorption temperature affected the equilibrium time. The adsorptivity of Cr(VI) on AC was found to be dependent on the initial concentration and the absorption temperature. The Cr(VI) equilibrium adsorption capacity, q_e (mg g^{-1}), was increased with increase in initial

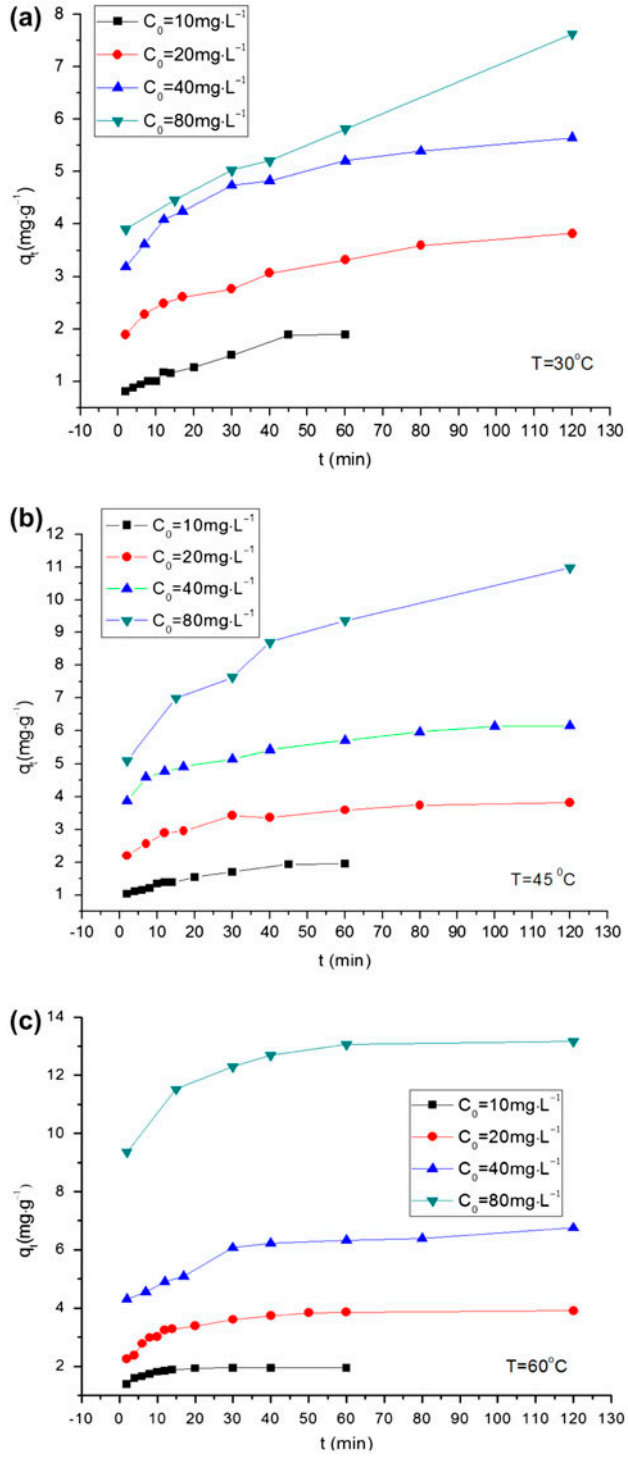

Fig. 2. Adsorption curves of chromium(VI) on AC uptake values at different initial concentrations and temperatures: (a) T = 30°C, (b) T = 45°C, and (c) T = 60°C.

concentration, and the absorption rate increased with increase in absorption temperature. This suggested that Cr(VI) adsorption from aqueous solutions onto AC was an endothermic process. The increase in the adsorption capacity may be due to the chemical interaction between Cr(VI) and AC, creation of some new adsorption sites or the increased rate of intraparticle diffusion of Cr(VI) into the pores of the AC at higher temperatures [36]. Furthermore, adsorption was rapid at the early stages and then gradually decreased and remained relatively constant after the equilibrium point. This study indicated that 60 min was needed to reach equilibrium. At low concentrations (10 mg L^{-1}), the ratio of available surface of AC to initial Cr(VI) was larger. However, the trends of q_e and p_t were completely different under higher concentrations of Cr(VI). For example, at 60°C, the percentage (p_t) of Cr(VI) adsorbed decreased from 99.10% to 85.18% as the Cr(VI) concentration increased from 10 to 80 mg L^{-1} and the amount of Cr(VI) adsorbed increased from 1.95 to 13.17 mg g^{-1}. That is, the amount of Cr(VI) adsorbed on the AC had a certain degree of saturation, which prevented further adsorption. Along with the data shown in Table 1, the curves also indicate that adsorption led to saturation, suggesting possible monolayer coverage of Cr(VI) on the surface of the AC.

3.2.3. Adsorption isotherms

To investigate the relationship between the amount of Cr(VI) adsorbed (q_e) and the aqueous concentration (C_e) at equilibrium, sorption isotherm models are usually employed for data fitting, of which the Langmuir and Freundlich equations are the most widely used. The Langmuir model assumes that the uptake of adsorbate molecules occurs on a homogenous surface by monolayer adsorption without any interaction between the adsorbed molecules [37]. The Freundlich model is suitable for non-ideal adsorption on heterogeneous surfaces. The heterogeneity is caused by the presence of different functional groups on the adsorbent surface and various adsorbent–adsorbate interactions [37]. To obtain the equilibrium data, the adsorbent mass 0.1 g, equilibrium time 2 h, and varied initial Cr(VI) concentrations (10, 20, 40, and 80 mg L^{-1}) were used for sorption experiments on the AC.

The Cr(VI) adsorption isotherm followed the linearized Freundlich model, as shown in Fig. 3. The relationship between the Cr(VI) uptake capacity, q_e (mg g^{-1}), of the AC and the residual Cr(VI) concentration, C_e (mg L^{-1}), at equilibrium is given by Eq. (4):

$$\ln q_e = \ln k_f + \frac{1}{n} \ln c_e \tag{4}$$

where the intercept $\ln k_f$ is a measure of adsorbent capacity, and the slope $1/n$ is the adsorption intensity. Generally, when the value of n is 2 to 10, it means that it is easy to adsorb; when n is less than 0.5, it is difficult to adsorb. According to the Freundlich theory, n can also be used to determine whether adsorption is favorable. When $n > 1$, adsorption is favorable, $n = 1$ indicates linear adsorption; and when $n < 1$, adsorption is unfavorable [38]. Freundlich equation constants and correlation coefficients (R^2) are given in Table 2. The isotherm data fit the Freundlich model (R^2 0.8537–0.9287). The constants k_f and n values were calculated to be 3.5509–5.0896 and 3.1260–4.7059, respectively, indicating a favorable adsorption process.

To ensure an equilibrium condition, the linear form of the Langmuir equation was applied to the experimental data. The Langmuir equation relates the quantity of Cr(VI) adsorbed per unit weight of adsorbent (mg g^{-1}) at equilibrium (q_e) to the equilibrium liquid concentration C_e (mg L^{-1}) by Eq. (5):

$$\frac{C_e}{q_e} = \frac{1}{q_{max} k_l} + \frac{C_e}{q_{max}} \tag{5}$$

Table 1
Equilibrium uptake capacities and adsorption yields obtained at different initial mass concentrations and temperatures

	30°C			45°C			60°C		
C_0 (mg L^{-1})	C_e (mg L^{-1})	q_e (mg g^{-1})	P_t (%)	C_e (mg L^{-1})	q_e (mg g^{-1})	P_t (%)	C_e (mg L^{-1})	q_e (mg g^{-1})	P_t (%)
10	0.08966	1.886	99.10	0.08966	1.951	99.13	0.08966	1.951	99.10
20	0.5878	3.825	97.06	0.3885	3.830	98.06	0.1893	3.915	99.05
40	10.94	5.648	72.65	8.149	6.149	79.63	5.160	6.752	87.10
80	40.74	7.630	49.07	24.81	10.97	69.00	11.85	13.17	85.18

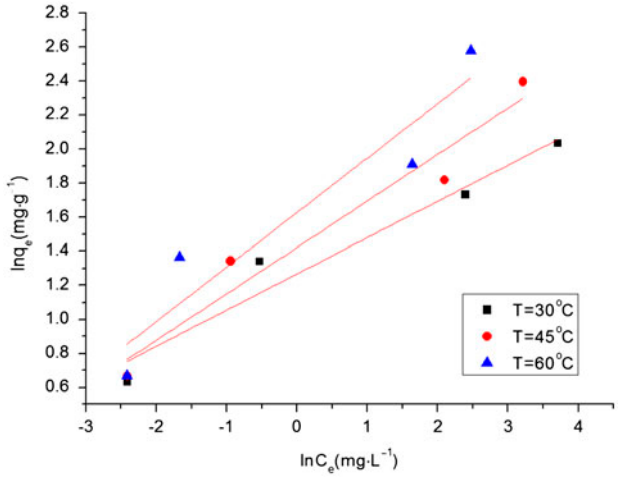

Fig. 3. Fitted Freundlich adsorption isotherms for chromium(VI) adsorption on AC.

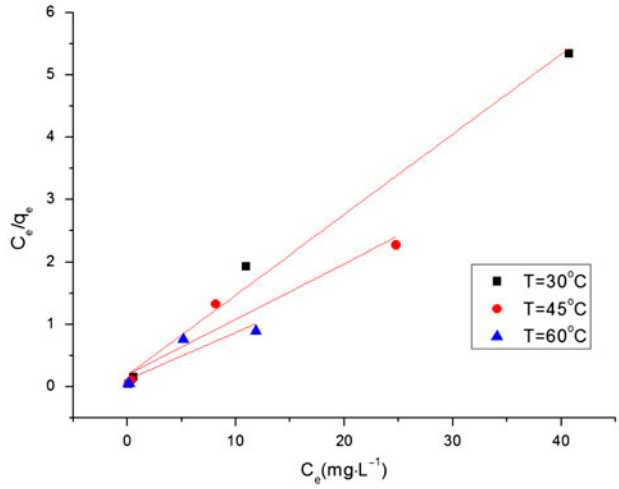

Fig. 4. Fitted Langmuir adsorption isotherms for chromium(VI) adsorption on AC.

where the constant q_{max} is the maximum single layer adsorption capacity (mg g^{-1}), and k_l is related to the free energy or adsorption enthalpy with respect to the closeness of active sites on the adsorbent surface with each other (L mg^{-1}).

Straight lines were obtained by plotting C_e/q_e against C_e as shown in Fig. 4, indicating the applicability of the Langmuir adsorption isotherm, which led to the conclusion that monolayer coverage of Cr(VI) adsorbate formed on the AC. The Langmuir constants q_{max} and k_l were calculated from the slopes and intercepts of plots of C_e/q_e vs. C_e, respectively, and correlation coefficients (R^2) are given in Table 2. It is clear that the maximum single layer adsorption capacity q_{max} values were higher at higher temperatures, reflecting the endothermic nature of Cr(VI) adsorption on AC.

The essential characteristics of the Langmuir isotherm can be expressed by a dimensionless equilibrium parameter, R_L, also known as the separation factor, defined by Weber and Chackravorti [37,39,40] as Eq. (6):

$$R_L = \frac{1}{1 + k_l C_0} \tag{6}$$

where k_l is the Langmuir constant and C_0 is the initial Cr(VI) concentration (mg L^{-1}). The R_L parameter gives important signs on the compatibility of adsorption for the selected adsorbent–adsorbate pair. There are four possibilities for the R_L value [39]: $0 < R_L < 1$, favorable adsorption; $R_L > 1$, unfavorable adsorption; $R_L = 1$, linear adsorption; and $R_L = 0$, irreversible adsorption. R_L values also indicate the type of isotherm. It is clear that the average values of R_L were between 0 and 1, indicating favorable adsorption of Cr(VI) on the AC samples.

Table 2
Isotherms constants for chromium(VI) adsorbed on AC

	Freundlich equation $\ln q_e = 1.2672 + 0.2125 \ln C_e$ (30°C) $\ln q_e = 1.4226 + 0.2728 \ln C_e$ (45°C) $\ln q_e = 1.6272 + 0.3199 \ln C_e$ (60°C)					Langmuir equation $C_e/q_e = 0.1839 + 0.1288\, C_e$ (30°C) $C_e/q_e = 0.1951 + 0.08877\, C_e$ (45°C) $C_e/q_e = 0.1111 + 0.07599\, C_e$ (60°C)			
Temperature (°C)	$\ln k_f$	k_f	$1/n$	n	R	q_{max}	k_l	R_L	R
30	1.2672	3.5509	0.2125	4.7059	0.9287	7.7640	0.7004	0.9747	0.9869
45	1.4226	4.1479	0.2728	3.6657	0.9231	11.2613	0.4637	0.9830	0.9007
60	1.6272	5.0896	0.3199	3.1260	0.8537	13.1519	0.6841	0.9753	0.7799

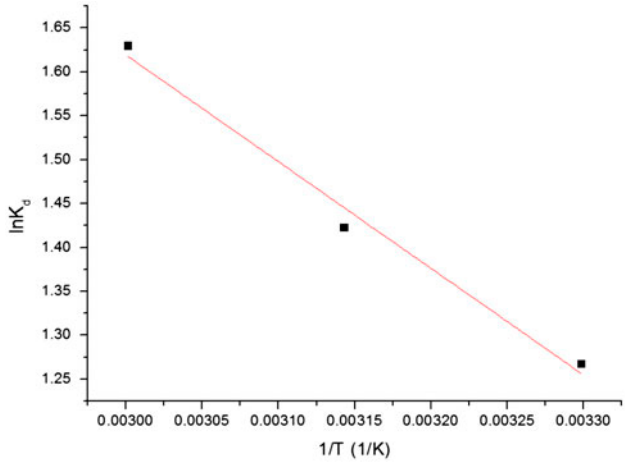

Fig. 5. Plot of $\ln K_d$ vs. $1/T$ for chromium(VI) adsorption on AC.

The Cr(VI) adsorption on AC process within the range of the selected conditions can be described approximately using the Langmuir and Freundlich isotherm equations. The Langmuir isothermal adsorption equation was better than the Freundlich adsorption isothermal equation at 30, 45, and 60°C, Freundlich adsorption isothermal equation was slightly better.

3.2.4. Adsorption thermodynamics parameters

ΔG° (Gibbs free energy change, kJ/mol) was calculated from the following Eqs. (7) and (8):

$$-\Delta G^{\circ} = RT \ln K_d \tag{7}$$

$$\Delta G^{\circ} = \Delta H^{\circ} - T\Delta S^{\circ} \tag{8}$$

The thermodynamic parameters such as ΔH° (enthalpy change, J mol^{-1}) and ΔS° (entropy change, J mol^{-1} K^{-1}) were calculated from the slopes and intercepts of the plots of $\ln K_d$ vs. $1/T$ as shown in Fig. 5, respectively, using Eq. (9):

$$\ln K_d = -\frac{\Delta H^{\circ}}{RT} + \frac{\Delta S^{\circ}}{R} \tag{9}$$

where R (8.314 J mol^{-1} K^{-1}) is the gas constant, T (K) is the absolute temperature, and K_d (L mg^{-1}) is the standard thermodynamic equilibrium constant defined by q_e/C_e, which is from the Langmuir equation (k_l) or Freundlich equation k_f. Because Cr(VI) adsorption data on the AC fit slightly better with the Freundlich adsorption isothermal equation in the study, the Freundlich adsorption isothermal constant was used.

The values of ΔH°, ΔS°, and ΔG° for Cr(VI) adsorption on AC are given in Table 3. The positive values of ΔH° indicated an endothermic process of adsorption, and the positive values of ΔS° showed that Cr(VI) adsorption caused disorder in the system. The value of ΔG° indicates the degree of spontaneity of an adsorption process, where a more negative value indicates an energetically favorable adsorption process. The increase in ΔG° with increasing temperature showed that adsorption was more favorable at high temperatures, similar to that reported by [37] for the adsorption of Cr(VI).

3.3. The kinetic study results of chromium(VI) adsorption on the prepared AC

It is important to predict the rate-limiting step in an adsorption process to understand the mechanism associated with the phenomena. For a solid–liquid adsorption process, the solute transfer is usually characterized by either external mass transfer or intraparticle diffusion or both [41]. Generally, three types of mechanisms are involved in an adsorption process: (1) film diffusion, which involves the movement of adsorbate molecules from the bulk of the solution toward the external surface of the adsorbent; (2) particle diffusion, where the adsorbate molecules move in the interior of the adsorbent particles; and (3) adsorption of the adsorbate molecules on the interior of the porous adsorbent [41]. Adsorption kinetics provide valuable information about controlling mechanisms of

Table 3
Adsorption thermodynamic parameters for chromium(VI) adsorbed on AC

K_d	Fitted linear equation $\ln K_d = -1215.73\frac{1}{T} + 5.2666$ (R^2=0.9764)				
	ΔS° (kJ mol^{-1})	ΔH° (kJ mol^{-1})	ΔG_1° (kJ mol^{-1}) (30°C)	ΔG_2° (kJ mol^{-1}) (45°C)	ΔG_3° (kJ mol^{-1}) (60°C)
k_f	43.7886	10.1081	−3.1665	−3.8233	−4.4801

adsorption processes, such as mass transfer or chemical reactions. The kinetics of Cr(VI) adsorption on AC was analyzed using pseudo-first-order, pseudo-second-order, and intraparticle diffusion models [37,42–44]. In pseudo-first-order and pseudo-second-order models, all of the adsorption steps, such as internal diffusion, external diffusion, and adsorption, were lumped together. It was assumed that the difference between the average solid phase concentration and the equilibrium concentration was the driving forces of adsorption, and the overall adsorption rate was proportional to either the driving force, as in the pseudo-first-order equation, or the square of the driving force, as in the pseudo-second-order equation [45]. Conformity between experimental data and the model-predicted values was expressed by the correlation coefficient (R^2). A relatively high R^2 value indicated that the model successfully described the kinetics of Cr(VI) adsorption [37].

3.3.1. Pseudo-first-order model

Lagergren proposed a pseudo-first-order kinetic model [46]. The integral form of the model is Eq. (10):

$$\ln(q_e - q_t) = \ln q_e - k_1 t \tag{10}$$

where q_t is the amount of Cr(VI) adsorbed (mg g^{-1}) at time t (min), q_e is the amount of Cr(VI) adsorbed at equilibrium (mg g^{-1}), and k_1 is the equilibrium rate constant of pseudo-first-order adsorption (min^{-1}).

Straight lines were obtained by plotting $\ln(q_e - q_t)$ against t as shown in Fig. 6 (a for 30℃, b for 45℃, and c for 60℃). The values of the rate constants k_1 and q_e were obtained from the slopes and intercepts of the plots, respectively (Table 4). The R^2 values obtained from the pseudo-first-order model were less than 0.9 at 30 and 45℃ and more than 0.9 at 60℃, which were higher than those from the intraparticle diffusion model and less than those from the pseudo-second-order model. The data indicated that adsorption of Cr(VI) on the AC could only be fit with good agreement to the pseudo-first-order model at 60℃ at relatively dilute solutions (Cr(VI) concentrations of 10 and 20 mg L^{-1}, R 0.9751 and 0.9933).

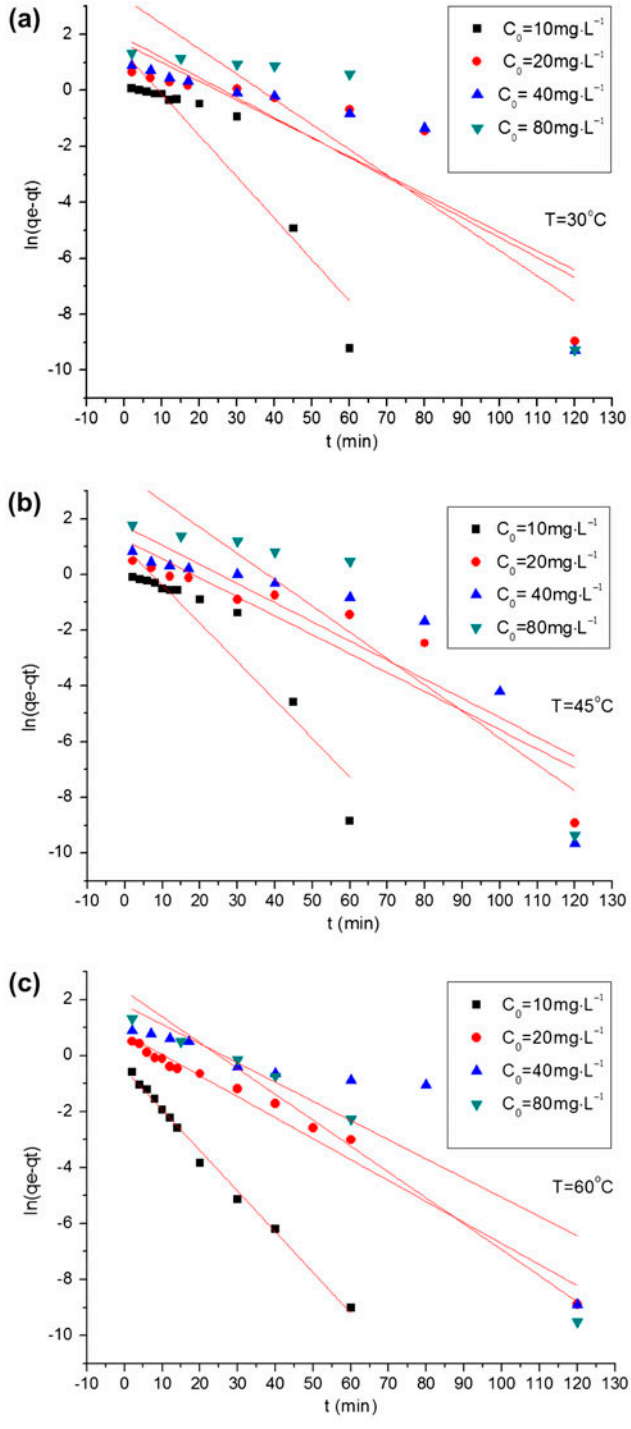

Fig. 6. The fitted straight line of pseudo-one-order model at different initial concentrations and temperatures: (a) T = 30℃, (b) T = 45℃, and (c) T = 60℃.

3.3.2. Pseudo-second-order model

The adsorption kinetics may also be described by a pseudo-second-order model. The linearized-integral form of the model is Eq. (11) [46]:

$$\frac{t}{q_t} = \frac{1}{k_2 q_e^2} + \frac{1}{q_e} t \tag{11}$$

Table 4
Kinetic parameters obtained for chromium(VI) adsorption on AC

		Pseudo-first-order model			Pseudo-second-order model			Intraparticle diffusion model		
T (℃)	C_0 (mg L^{-1})	k_1	q_e	R^2	k_2	q_e	R^2	k_{id}	c	R^2
30	10	0.1480	3.8415	0.8588	0.1463	1.6158	0.9703	0.1884	0.4868	0.9715
	20	0.06745	5.3364	0.7357	0.03262	3.9442	0.9901	0.2008	1.7327	0.9830
	40	0.07141	6.5549	0.7503	0.03348	5.7800	0.9971	0.2587	3.0830	0.9440
	80	0.09015	26.7026	0.7751	0.009191	8.0038	0.9520	0.3873	3.0340	0.9445
45	10	0.1375	2.6916	0.8782	0.09176	2.0940	0.9911	0.1594	0.8023	0.9778
	20	0.06818	3.4427	0.8241	0.05910	3.9271	0.9982	0.1694	2.2134	0.8936
	40	0.06889	5.6773	0.7613	0.03764	6.3008	0.9977	0.2257	3.8878	0.9522
	80	0.09457	36.2116	0.8161	0.008606	11.5287	0.9828	0.6159	4.4560	0.9811
60	10	0.1452	0.6138	0.9933	0.5299	1.9920	0.9999	0.1799	2.4085	0.7676
	20	0.07501	2.1932	0.9751	0.08966	4.0098	0.9997	0.2766	4.0562	0.8829
	40	0.06868	6.0716	0.7506	0.03575	6.8705	0.9981	0.3886	9.7007	0.7398
	80	0.09253	10.1411	0.9554	0.04051	13.3618	0.9997	0.07776	1.4861	0.6602

where k_2 is the pseudo-second-order rate constant of adsorption.

The linear plot of t/q_t vs. t gave $1/q_e$ as the slope and $1/k_2q_e^2$ as the intercept. Fig. 7 (a for 30℃, b for 45℃, and c for 60℃) shows good agreement between the experimental and the calculated q_e values. From Table 4, all of the R^2 values obtained from the pseudo-second-order model were more than 0.95, indicating that the model accurately characterized the adsorption of Cr(VI) on the AC under the conditions tested.

3.3.3. Intraparticle diffusion model

An intraparticle diffusion model is of major concern because it is the rate-determining step in the liquid–solid adsorption systems. During the batch mode of operation, there is a possibility of transport of sorbate species into the pores of sorbent, which is often a rate-controlling step. An intraparticle diffusion model, based on the theory proposed by Weber and Morris [47,48], was used to identify the diffusion mechanisms. The model featured an empirical functional relationship, common to most adsorption processes, where uptake varies proportionally with $t^{1/2}$ rather than with the contact time, t. The intraparticle diffusion equation is expressed as Eq. (12):

$$q_t = k_{id}t^{1/2} + c \quad (12)$$

where k_{id} (mg g^{-1} $min^{-1/2}$) is the intraparticle diffusion rate constant, and c is the intercept (mg g^{-1}).

The plot of q_t vs. $t^{1/2}$ gave straight lines, and the values of k_{id} were calculated from the slopes of the plots. The values of c gave an idea about the thickness of boundary layer, i.e., the larger the intercept, the greater the contribution of surface sorption in the rate-controlling step. The adsorption of Cr(VI) on AC with the intraparticle diffusion model is shown in Fig. 8 (a for 30℃, b for 45℃, and c for 60℃), and the relative parameters are given in Table 4. The R^2 values obtained at 30 and 45°C are higher than 0.94 (except for initial concentration 20 mg L^{-1} at 45℃) and less than 0.88 at 60℃, indicating that the adsorption of Cr (VI) on AC could only be described by the intraparticle diffusion model at lower temperatures (30 and 45℃).

The values of the correlation coefficient (R^2) of pseudo-first-order, pseudo-second-order and intraparticle diffusion kinetic models showed that Cr(VI) adsorption on AC followed the pseudo-second-order model at 30, 45, and 60℃ (R 0.9520–0.9999), the intraparticle diffusion model at lower temperatures (30 and 45℃, R 0.8936–0.9830), and only followed the pseudo-first-order equation at 60℃ at relatively dilute solutions (Cr(VI) concentrations of 10 and 20 mg L^{-1}, R 0.9751 and 0.9933). In short, pseudo-second-order kinetic equations had higher R^2 values among these three models. Therefore, the pseudo-second-order kinetic model was taken as the most appropriate model for description of the adsorption mechanism of Cr(VI) on the prepared AC.

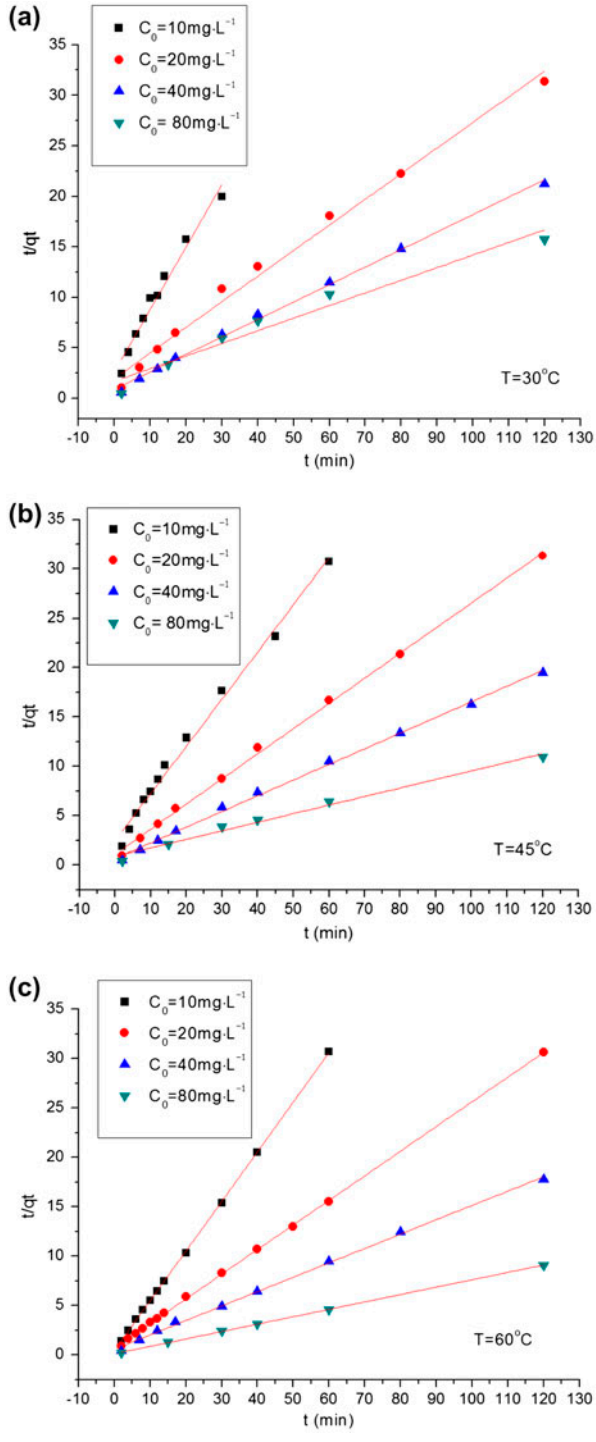

Fig. 7. The fitted straight line of pseudo-second-order model at different initial concentrations and temperatures: (a) T = 30℃, (b) T = 45℃, and (c) T = 60℃.

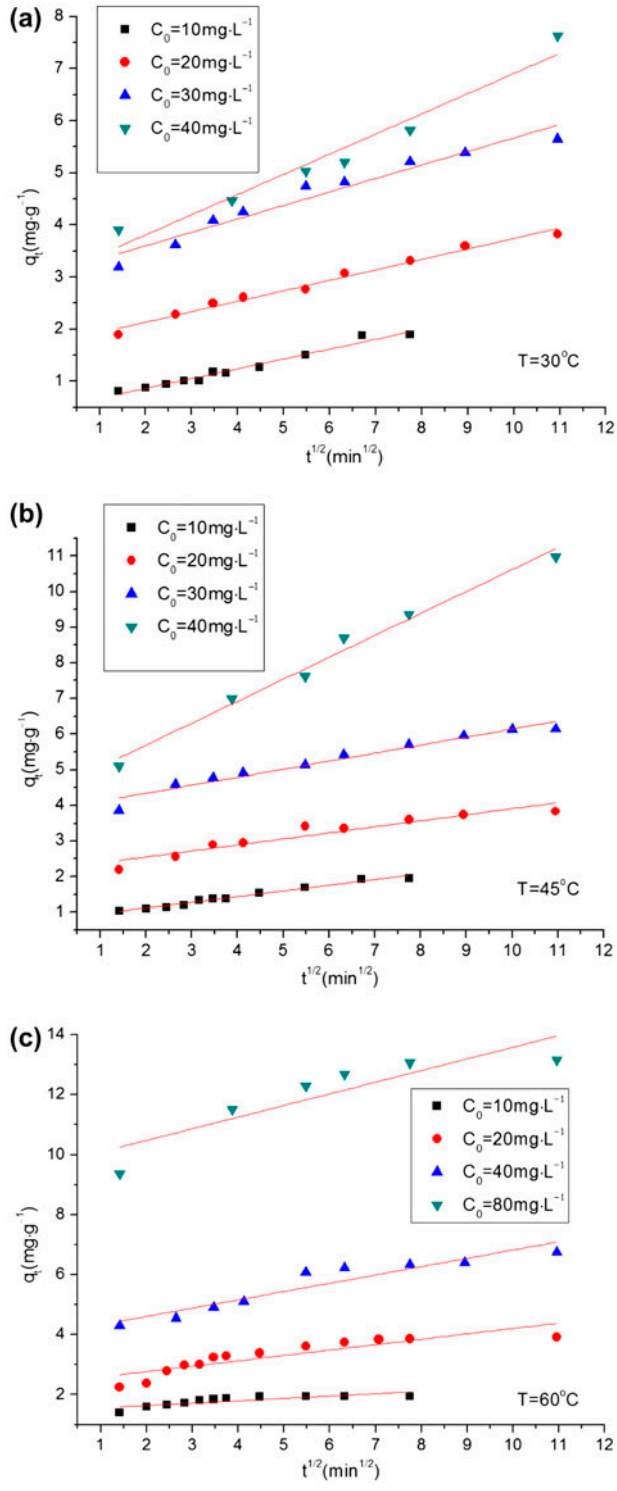

Fig. 8. Intraparticle diffusion kinetic plot at different initial concentrations and temperatures: (a) T = 30℃, (b) T = 45℃, and (c) T = 60℃.

4. Conclusions

AC was prepared from ES by microwave-assisted activation with $ZnCl_2$. The prepared AC was characterized for absorption capacity, surface area, pore volume, and surface functional groups. The AC was used for removal of Cr(VI) from aqueous solutions with concentrations ranging from 10 to 80 mg L^{-1} and temperatures between 30 and 60℃. The effects of pH, contact time, initial concentration of Cr(VI) and temperature on adsorption, as well as the thermodynamics and kinetics of Cr(VI) adsorption on the prepared AC were investigated. The results are summarized as follows:

(1) The methylene blue adsorption capacity, iodine number, phenol adsorption capacity, Cr(VI) adsorption capacity, and BET surface area of the prepared AC were 277.5, 1,041.5, 104.3, 6.29, and 1,429.4 m g^{-1}, respectively. The total pore volume, micropore volume, and average pore diameter of AC were 1.105, 0.008403 cm^3 g^{-1} and 3.09 nm, respectively. Carbonyl and hydroxyl groups were found on the AC surface.
(2) The adsorption capacity of Cr(VI) was dependent on pH and initial concentration: equilibrium time increased but the Cr(VI) removal percentage decreased with an increase in the initial Cr(VI) concentration.
(3) Isotherm data were treated according to the Langmuir and Freundlich models and showed that adsorption of Cr(VI) on AC was in good agreement with the Langmuir adsorption isotherm model at 30℃ (R = 0.9869) and the Freundlich adsorption isotherm model at 45℃ (R = 0.9287) and 60℃ (R = 0.9231).
(4) Adsorption thermodynamic parameters for Cr (VI) adsorbed on the AC, namely ΔH° (10.1081 kJ mol^{-1}), ΔS° (43.7886 kJ mol^{-1} K^{-1}), and ΔG° (−3.1665 kJ mol^{-1}, 30℃; −3.8233 kJ mol^{-1}, 45℃; −4.4801 kJ mol^{-1}, 60℃), indicated that the adsorption was a spontaneous and endothermic process with increased randomness at the solid–solution interface.
(5) Adsorption kinetics of Cr(VI) were analyzed by pseudo-first-order, pseudo-second-order, and intraparticle diffusion kinetic models, and the results showed that Cr(VI) adsorption on AC followed the pseudo-second-order model at 30, 45, and 60℃ (R 0.9520–0.9999), the intraparticle diffusion model at lower temperatures (30 and 45℃, R 0.8936–0.9830), and only followed the pseudo-first-order equation at 60℃ at relatively dilute solutions (Cr(VI) concentrations of 10 and 20 mg L^{-1}, R 0.9751, and 0.9933). The pseudo-second-order kinetic model provided the best fit, indicating that it is most appropriate for description of the adsorption mechanism of Cr(VI) on the prepared AC.

Acknowledgments

The authors are grateful for the financial support from the National Natural Science Foundation of China (No. 21266002). This project was also supported by Guangxi University and Guangxi Education Department Education Reform in the twenty-first Century Research Fund of China (No. 2011JGA010), the Dean Project of Guangxi Key Laboratory of Petrochemical Resource Processing and Process Intensification Technology of China (No. 2014K006), and the Scientific Research Foundation of Guangxi University (No. XBZ110639).

References

[1] P. Miretzky, A.F. Cirelli, Cr(VI) and Cr(III) removal from aqueous solution by raw and modified lignocellulosic materials: A review, J. Hazard. Mater. 180 (2010) 1–19.
[2] V. Sarin, T.S. Singh, K.K. Pant, Thermodynamic and breakthrough column studies for the selective sorption of chromium from industrial effluent on activated eucalyptus bark, Bioresour. Technol. 97 (2006) 1986–1993.
[3] F. Richard, A. Bourg, Aqueous geochemistry of chromium: A review, Water Res. 25 (1991) 807–816.
[4] USEPA, USEPA Drinking Water Regulations and Health Advisories, EPA 822-B-96-002, USEPA, Washington, DC, 1996.
[5] WHO, Guidelines for Drinking Water Quality. Health Criteria and Other Supporting Information, vol. 1, second ed., World Health Organization, Geneva, Switzerland, 1997.
[6] D. Mohan, C. Pittman Jr., Activated carbons and low cost adsorbents for remediation of tri-and hexavalent chromium from water, J. Hazard. Mater. 137 (2006) 762–811.
[7] IARC (International Agency for Research on Cancer), IARC Monographs on the Evaluation of Carcinogenic Risks to Humans: Overall Evaluation of Carcinogenicity. An Updating of IARC Monographs, vols. 1–42, Supplement 7, WHO, Lyon, France, 1987.
[8] M. Cieślak-Golonka, Toxic and mutagenic effects of chromium(VI). A review, Polyhedron 15 (1996) 3667–3689.
[9] K.K. Krishnani, S. Ayyappan, Heavy metals remediation of water using plants and lignocellulosic agrowastes, Rev. Environ. Contam. Toxicol. 188 (2006) 59–84.
[10] J. Kotaś, Z. Stasicka, Chromium occurrence in the environment and methods of its speciation, Environ. Pollut. 107 (2000) 263–283.

[11] M. Gheju, I. Balcu, Removal of chromium from Cr(VI) polluted wastewaters by reduction with scrap iron and subsequent precipitation of resulted cations, J. Hazard. Mater. 196 (2011) 131–138.
[12] P. Religa, A. Kowalik-Klimczak, P. Gierycz, Study on the behavior of nanofiltration membranes using for chromium(III) recovery from salt mixture solution, Desalination 315 (2013) 115–123.
[13] A. Senol, Amine extraction of chromium(VI) from aqueous acidic solutions, Sep. Purif. Technol. 36 (2004) 63–75.
[14] S. Mustafa, K.H. Shah, A. Naeem, M. Waseem, M. Tahir, Chromium(III) removal by weak acid exchanger Amberlite IRC-50 (Na), J. Hazard. Mater. 160 (2008) 1–5.
[15] P. Rana, N. Mohan, C. Rajagopal, Electrochemical removal of chromium from wastewater by using carbon aerogel electrodes, Water Res. 38 (2004) 2811–2820.
[16] Y.X. Liu, D.X. Yuan, J.M. Yan, Electrochemical removal of chromium from aqueous solutions using electrodes of stainless steel nets coated with single wall carbon nanotubes, J. Hazard. Mater. 186 (2011) 473–480.
[17] Y. Chen, G. Gu, Preliminary studies on continuous chromium(VI) biological removal from wastewater by anaerobic–aerobic activated sludge process, Bioresour. Technol. 96(15) (2005) 1713–1721.
[18] W. Li, Y.K. Tang, Y.T. Zeng, Z.F. Tong, D.W. Liang, W. Cui, Adsorption behavior of Cr(VI) ions on tannin-immobilized activated clay, Chem. Eng. J. 193–194 (2012) 88–95.
[19] B. Saha, C. Orvig, Biosorbents for hexavalent chromium elimination from industrial and municipal effluents, Coord. Chem. Rev. 254 (2010) 2959–2972.
[20] Y. Chen, Y.C. Zhu, Z.C. Wang, Y. Li, L.L. Wang, L.L. Ding, X.Y. Gao, Y.J. Ma, Y.P. Guo, Application studies of activated carbon derived from rice husks produced by chemical-thermal process—A review, Adv. Colloid Interface Sci. 163 (2011) 39–52.
[21] J.M. Dias, M.C.M. Alvim-Ferraz, M.F. Almeida, J. Rivera-Utrilla, M. Sánchez-Polo, Waste materials for activated carbon preparation and its use in aqueous-phase treatment: A review, J. Environ. Manage. 85 (2007) 833–846.
[22] N.M. Nor, L.L. Chung, L.K. Teong, A.R. Mohamed, Synthesis of activated carbon from lignocellulosic biomass and its applications in air pollution control—A review, J. Environ. Chem. Eng. 1 (2013) 658–666.
[23] J. Rivera-Utrilla, M. Sánchez-Polo, V. Gómez-Serrano, P.M. Álvarez, M.C.M. Alvim-Ferraz, J.M. Dias, Activated carbon modifications to enhance its water treatment applications.An overview, J. Hazard. Mater. 187 (2011) 1–23.
[24] J. Acharya, J.N. Sahu, B.K. Sahoo, C.R. Mohanty, B.C. Meikap, Removal of chromium(VI) from wastewater by activated carbon developed from *Tamarind wood* activated with zinc chloride, Chem. Eng. J. 150 (2009) 25–39.
[25] H. Zhang, Y. Tang, D.Q. Cai, X.N. Liu, X.Q. Wang, Q. Huang, Z.L. Yu, Hexavalent chromium removal from aqueous solution by algal bloom residue derived activated carbon: Equilibrium and kinetic studies, J. Hazard. Mater. 181 (2010) 801–808.
[26] Y.Y. Sun, Q.Y. Yue, B.Y. Gao, Y. Gao, Q. Li, Y. Wang, Adsorption of hexavalent chromium on *Arundo donax Linn* activated carbon amine-crosslinked copolymer, Chem. Eng. J. 217 (2013) 240–247.
[27] J.B. Yang, M.Q. Yu, W.T. Chen, Adsorption of hexavalent chromium from aqueous solution by activated carbon prepared from longan seed: Kinetics, equilibrium and thermodynamics, J. Ind. Eng. Chem. 21 (2015) 414–422.
[28] F. Di Natale, A. Erto, A. Lancia, D. Musmarra, Equilibrium and dynamic study on hexavalent chromium adsorption onto activated carbon, J. Hazard. Mater. 281 (2015) 47–55.
[29] G.H. Jing, Z.M. Zhou, L. Song, M.X. Dong, Ultrasound enhanced adsorption and desorption of chromium(VI) on activated carbon and polymeric resin, Desalination 279 (2011) 423–427.
[30] C.J. Chen, P.C. Zhao, Y.M. Huang, Z.F. Tong, Z.X. Li, Preparation and characterization of activated carbon from eucalyptus sawdust I. activated by NaOH, J. Inorg. Organomet. Polym. Mater. 23 (2013) 1201–1209.
[31] H. Demiral, İ. Demiral, F. Tümsek, B. Karabacakoğlu, Adsorption of chromium(VI) from aqueous solution by activated carbon derived from olive bagasse and applicability of different adsorption models, Chem. Eng. J. 144 (2008) 188–196.
[32] N.V. Vivek Narayanan, M. Ganesan, Use of adsorption using granular activated carbon (GAC) for the enhancement of removal of chromium from synthetic wastewater by electrocoagulation, J. Hazard. Mater. 161 (2009) 575–580.
[33] A. Sharma, K.G. Bhattacharyya, Adsorption of chromium(VI) on *Azadirachta indica* (neem) leaf powder, Adsorption 10 (2004) 327–338.
[34] V.K. Singh, P.N. Tiwari, Removal and recovery of chromium(VI) from industrial waste water, J. Chem. Technol. Biotechnol. 69 (1997) 376–382.
[35] M. Rao, A.V. Parwate, A.G. Bhole, Removal of Cr^{6+} and Ni^{2+} from aqueous solution using bagasse and fly ash, Waste Manage. 22 (2002) 821–830.
[36] K. Anupam, S. Dutta, C. Bhattacharjee, S. Datta, Adsorptive removal of chromium(VI) from aqueous solution over powdered activated carbon: Optimisation through response surface methodology, Chem. Eng. J. 173 (2011) 135–143.
[37] Z.A. AL-Othman, R. Ali, M. Naushad, Hexavalent chromium removal from aqueous medium by activated carbon prepared from peanut shell: Adsorption kinetics, equilibrium and thermodynamic studies, Chem. Eng. J. 184 (2012) 238–247.
[38] T. Qiu, Y. Zeng, C.S. Ye, H. Tian, Adsorption thermodynamics and kinetics of *p*-Xylene on activated carbon, J. Chem. Eng. Data 57 (2012) 1551–1556.
[39] A. Gundogdu, C. Duran, H.B. Senturk, M. Soylak, D. Ozdes, H. Serencam, M. Imamoglu, Adsorption of phenol from aqueous solution on a low-cost activated carbon produced from tea industry waste: Equilibrium, kinetic, and thermodynamic study, J. Chem. Eng. Data 57 (2012) 2733–2743.
[40] T.W. Weber, R.K. Chakravorti, Pore and solid diffusion models for fixed-bed adsorbers, J. Am. Inst. Chem. Eng. 20 (1974) 228–238.
[41] P. Chingombe, B. Saha, R.J. Wakeman, Sorption of atrazine on conventional and surface modified

activated carbons, J. Colloid Interface Sci. 302 (2006) 408–416.
[42] M. Naushad, M.A. Khan, Z.A. Alothman, M.R. Khan, Adsorptive removal of nitrate from synthetic and commercially available bottled water samples using De-Acidite FF-IP resin, J. Ind. Eng. Chem. 20 (2014) 3400–3407.
[43] M. Naushad, Surfactant assisted nano-composite cation exchanger: Development, characterization and applications for the removal of toxic Pb^{2+} from aqueous medium, Chem. Eng. J. 235 (2014) 100–108.
[44] S.M. Alshehri, M. Naushad, T. Ahamad, Z.A. Alothman, A. Aldalbahi, Synthesis, characterization of curcumin based ecofriendly antimicrobial bio-adsorbent for the removal of phenol from aqueous medium, Chem. Eng. J. 254 (2014) 181–189.
[45] Y.S. Ho, G. McKay, Sorption of dye from aqueous solution by peat, Chem. Eng. J. 70 (1998) 115–124.
[46] M.A. Ahmad, R. Alrozi, Removal of malachite green dye from aqueous solution using rambutan peel-based activated carbon: Equilibrium, kinetic and thermodynamic studies, Chem. Eng. J. 171 (2011) 510–516.
[47] C.H. Weng, Y.T. Lin, T.W. Tzeng, Removal of methylene blue from aqueous solution by adsorption onto pineapple leaf powder, J. Hazard. Mater. 170 (2009) 417–424.
[48] I.A.W. Tan, A.L. Ahmad, B.H. Hameed, Adsorption of basic dye on high-surface-area activated carbon prepared from coconut husk: Equilibrium, kinetic and thermodynamic studies, J. Hazard. Mater. 154 (2008) 337–346.